Journal of Comparative Physiology A (2020) 206:45–54
https://doi.org/10.1007/s00359-019-01386-6

ORIGINAL PAPER

Intracranial pressure in the American Alligator (*Alligator mississippiensis*): reptilian meninges and orthostatic gradients

Tatyana Kondrashova[1] · Joshua Blanchard[2] · Lucas Knoche[3] · James Potter[4] · Bruce A. Young[3]

Received: 16 February 2019 / Revised: 16 November 2019 / Accepted: 26 November 2019 / Published online: 6 December 2019
© Springer-Verlag GmbH Germany, part of Springer Nature 2019

Abstract

The cranial meninges of reptiles differ from the more widely studied mammalian pattern in that the intraventricular and subarachnoid spaces are, at least partially, isolated. This study was undertaken to investigate the bulk flow of cerebrospinal fluid, and the resulting changes in intracranial pressure, in a common reptilian species. Intracranial pressure was measured using ocular ultrasonography and by surgically implanting pressure cannulae into the cranial subarachnoid space. The system was then challenged by: rotating the animal to create orthostatic gradients, perturbation of the vascular system, administration of epinephrine, and cephalic cutaneous heating. Pressure changes determined from the implanted catheters and through quantification of the optic nerve sheath were highly correlated and showed a significant linear relationship with orthostatic gradients. The catheter pressure responses were phasic, with an initial rapid response followed by a much slower response; each phase accounted for roughly half of the total pressure change. No significant relationship was found between intracranial pressure and either heart rate or blood flow. The focal application of heat and the administration of epinephrine both increased intracranial pressure, the latter influence being particularly pronounced.

Keywords Optic nerve sheath · Barostatic reflex · Ocular ultrasonography · Cerebrospinal fluid · Reptile

Abbreviations

CSF	Cerebrospinal fluid
EKG	Electrocardiogram
ICP	Intracranial pressure

Introduction

In humans, elevated intracranial pressure (ICP) is an important cause of secondary brain injury or even death (Jagannathan et al. 2008; Ferguson et al. 2016). The most reliable and accurate way of assessing ICP is by surgically implanting a catheter (typically intraventricularly) connected to a pressure transducer (Carney et al. 2017). The invasive nature of this procedure, coupled with the potential for hemorrhage and infection, has motivated workers to find indirect means of assessing ICP. The optic nerve is surrounded by a layer of connective tissue (the optic nerve sheath) that is continuous with the dura mater of the brain. There is cerebrospinal fluid (CSF) within the optic nerve sheath that is continuous with the CSF in the subarachnoid space (Killer et al. 2003). Increases in ICP lead to linear increases in fluid pressure within the optic nerve sheath and, ultimately, the distension of the sheath (Liu and Kahn 1993; Hansen and Helmke 1996). Quantifying the diameter of the optic nerve sheath using ocular ultrasonography produces values that are strongly correlated with catheter-measured ICP (Rajajee et al. 2011; Strumwasser et al. 2011; Fernando et al. 2019).

Ocular ultrasonography is widely used in clinical settings to assess ICP in humans (Komut et al. 2016; Raffiz and Abdullah 2017), and has been used in this capacity with other mammals (Cooley et al. 2015; Yang et al. 2017; Smith et al. 2018). Applying this technique to other vertebrates may be challenging given the differences in the meninges and CSF circulatory dynamics. The study of the reptilian meninges has produced an abundance of contradictory results and conflicting

✉ Bruce A. Young
byoung@atsu.edu

[1] Department of Family Medicine, Preventive Medicine, and Community Health, Kirksville College of Osteopathic Medicine, A.T. Still University, Kirksville, MO, USA

[2] Department of Anesthesiology, Northeast Regional Medical Center, Kirksville, MO, USA

[3] Department of Anatomy, Kirksville College of Osteopathic Medicine, A.T. Still University, Kirksville, MO, USA

[4] Department of Surgery, Kirksville College of Osteopathic Medicine, A.T. Still University, Kirksville, MO, USA

nomenclature. Earlier workers (Ariens Kappers 1926) generally argued for the lack of an arachnoid in reptiles. Contemporaneous works approaching the subject from the perspectives of embryology (Stark 1969) or histology (Zajicova 1975) produced contradictory findings. Herein, we will follow (Zajicova 1975) in recognizing a reptilian arachnoid that is isolated from the pia by a fluid-filled subarachnoid space. Reptiles have a well-developed ventricular system that is proportionately larger than the mammalian system, and includes proportionately larger choroid plexi (Cserr and Bundgaard 1984). In *Alligator* and other reptiles, there are no large continuities or portals between the ventricular system and the subarachnoid space; indeed, several workers have argued that the subarachnoid fluid surrounding the brain was distinct from the CSF located within the ventricles (Ariens Kappers et al. 1960). Tracer studies have shown that these two fluids intermix (Heisey 1970), presumably through small pores in the roof of the 4th ventricle (Jones 1978). Given the unusual nature of the arachnoid in *Alligator*, it remains unclear how CSF is "recycled" into the bloodstream in these reptiles.

The relative isolation of the ventricular CSF from the subarachnoid CSF in *Alligator* suggests that these animals may respond differently, at least temporally, to alterations of ICP. This study was designed to test the hypothesis that while both ICP and optic nerve sheath diameter would change in response to orthostatic gradients, the two would exhibit different temporal patterns of change. The (reportedly avascular) arachnoid morphology of reptiles has been interpreted as a barrier, rather than exchange, specialization (Zajicova 1975), suggesting that the dynamics between the CSF and the blood may be different in reptiles. Understanding the dynamics between ICP, CSF movement, and the venous system is further complicated by the presence of multiple venous shunts in the head of *Alligator* which likely serve an active thermoregulatory function (Porter et al. 2016). A recent study demonstrated that orthostatic gradients do not trigger a baroreflex in *A. mississippiensis*; instead, these gradients lead to marked swings in cephalic blood pressure (Knoche et al. 2019). We hypothesize that in *Alligator*, contrary to most vertebrates, there is little short-term relationship between blood flow and ICP; we explored this hypothesis by measuring ICP (directly and indirectly), while altering blood flow patterns through changes in posture, heart rate, vascular occlusion, the application of heat, and the administration of epinephrine.

Materials and methods

Live animals

Five live sub-adult (165–183 cm total length, mass 9.7–17.5 kg) American alligators (*Alligator mississippiensis*) were obtained from the Louisiana Department of Wildlife and Fisheries. The animals were housed communally in a 29 m^2 facility that featured three submerging ponds, natural light, and artificial lights on a 12:12 cycle. The facility was maintained at 30–33 °C, and warm water rain showers were provided every 20 min, which helped maintain the facility at > 75% relative humidity. The alligators were maintained on a diet of previously frozen adult rats. When the individual animals were removed from the enclosure, they were caught by noosing, their jaws taped shut using vinyl tape, and their fore limbs and hind limbs taped in a retracted position.

Gravitational gradients

Each individual, un-anesthetized and bound as described above, was placed on a stiff board (244 × 28 × 3.8 cm thick), which exceeded the maximum width and length of the alligators used for this study. Six 2.5 cm-wide heavy duty straps (Northwest Tarp and Canvas; Bellingham, WA) were used to secure the alligator to the board; the straps were tight enough to minimize movement of the animal, but not tight enough to impede ventilation or circulation. The board was anchored to a rotating spindle machined to have, in addition to a stable horizontal stop, fixed "stops" at 15°, 30°, and 45° above and below the horizon.

Non-invasive trials

Individual alligators were placed on the rotating board, but were not exposed to any anesthesia or chemical agent. The animals were subjected to either 90 or 240 s rotation trials, with the direction and magnitude of the rotation determined by die roll. During the rotations, the alligator's electrocardiograms (EKGs) were recorded using two silver chloride surface cup electrodes (019-477200, GRASS, Natus Medical, Pleasanton, CA), coated with a layer of conducting gel (Signagel, Parker Laboratories, Fairfield, NJ) and placed on the ventral surface of the animal on either side of the heart. The electrodes were connected to a preamplifier (P511, GRASS) and the EKG signal recorded (at 1.0 kHz) using a MiDAS (Xcitex Inc., Woburn, MA) data acquisition system. Simultaneously, ocular ultrasonography was performed using a portable ultrasound machine (Shenzhen Mindray-M7, Bio-medical Electronics Co.). The optic nerve was imaged using a linear array probe (L12-4s; Shenzhen Mindray Bio-Medical Electronics Co.) placed directly against the cornea or eyelid using ultrasound gel. The ultrasound images were imported into ImageJ (NIH) and the diameter of the optic nerve quantified. The optic nerve was measured in a region centered 4 mm proximal to the retina (following Hansen et al. 1994).

A 0.75 mm probe was inserted into the alligator's external nares and then connected to a TC-1000 thermometer (CWE,

Inc.), which was, in turn, connected to the MiDAS data-acquisition system. An electric heating pad was placed on the dorsum of the alligator's snout, cranial to the orbit, but caudal to the probe and the external nares. At the end of the non-invasive trials, epinephrine (at 0.1 mg/kg) was administered into the triceps of each alligator (following Gatson et al. 2017), while the effect on ICP was determined with ocular ultrasonography.

Invasive trials

Following a minimum of a 2-week recovery period, each alligator was noosed and induced to bite a soft bite pad, which (when taped in place) enabled safe intubation. A cuffed tracheal tube was connected to a custom anesthesia system that included a ventilator pump (Harvard), Vaporstick anesthesia machine (Surgivet), isoflurane vaporizer (Surgivet), and Capnomac Ultima respiratory gas monitor (Datex-Engstrom). The alligators were maintained on a steady ventilatory pattern of 6 or 8 breaths per minute (depending on size) each with a tidal volume of 500 ml; this ventilatory rate matches what has been reported from non-anesthetized alligators (e.g., Claessens 2009; Brocklehurst et al. 2017), and tracking CO_2 in the exhaled gas allowed for adjustments to prevent hypocapnia. Anesthetic induction was accomplished using 5% isoflurane, once a surgical plane of anesthesia was established the animal was maintained on 1.5–3% isoflurane depending on the responses of the individual alligator.

Once a surgical plane of anesthesia was established, analgesic (Meloxicam at 0.2 mg/kg) and antibiotic (Amikacin at 5 mg/kg) were administered IM into the triceps. The animal was positioned supine, and a surgical incision made along the ventral midline of the caudal lower jaw and throat. Through this incision, the common carotid artery (distal to the branching from the single primary carotid in *Alligator*) and jugular vein were surgically isolated on the animal's right side. The animals were returned to a prone position, and then, EKG and ocular ultrasound data recorded (as detailed above) with and without vascular clamps occluding the exposed vessels; the ocular ultrasonography was performed ipsilateral to the occluded vessels. To minimize risk to the subject, rotations were restricted to 15°, while the vessels were occluded; EKG and ocular ultrasonography were performed during the rotations. Following a series of rotations, and data collection, the incision was closed with suture and cyanoacrylate surgical adhesive.

A stainless steel surgical burr was used to bore through the dorsum of the alligator's skull. Using published 3-D reconstructions (Witmer and Ridgely 2008) and preserved material as guides, an approximately 4 mm-diameter portal through the sagittal midline of the skull was bored just caudal to the orbits. This allowed for direct exposure of the dura mater; a small incision in the dura was used to inset a segment of PE tubing into the subarachnoid space. The PE tubing was connected to a P23BB fluid pressure transducer (Gould), both of which were filled with reptilian Ringer's solution. The pressure transducer was mounted to the rotating board at a fixed site immediately adjacent to the alligator's head, so that rotation of the alligator did not produce a pressure head between the PE tubing and the transducer. The implantation of the PE tubing was snug enough that no CSF leakage was observed, yet the functionality of the coupling was evident by the (pressure-driven) movement of the yellowish CSF along a distance of the PE tubing. The pressure transducer was coupled to a P122 preamplifier (GRASS) and then to the data-acquisition system (MiDAS, Xcitex). Signals from the pressure transducer were recorded simultaneously with EKG and ocular ultrasonography (as described above).

Upon the completion of this data collection, the PE tubing was removed from the subarachnoid space. The incision in the dura was sealed with cyanoacrylate adhesive, and then, the opening in the skull filled with epoxy cement. As the alligator was recovering from anesthesia 0.1 mg/kg of epinephrine was injected into the triceps, additional ocular ultrasonography performed. All of the alligators recovered completely from the procedures.

Morphology

The eye and associated contents of the orbit were excised from the head of a previously preserved 1.8 m (total length) specimen of *Alligator mississippiensis*. The excised tissue was dehydrated through an ethanol series, embedded in Paraplast, and then frontal sections cut at 10 µm. Mounted sections were stained with hematoxylin and eosin, and then digitally photographed using a DM 4000B microscope (Leica Microsystems, Inc.).

Results

In frontal sections (Fig. 1a) and corneal sonographic images (Fig. 1b), the long axis of the optic nerve can be followed through the orbit. The nerve was surrounded by a prominent optic nerve sheath composed of type 1 collagen with a scalloped appearance in section; histological assay found no evidence of elastin within the sheath. The sheath and nerve were separated by a fluid-filled space that was continuous with the cranial subarachnoid space. The optic nerve sheath attached to the external surface of the sclera (which is largely cartilaginous in *Alligator*), flaring out over the medial surface of the eye. The optic nerve, and nerve sheath,

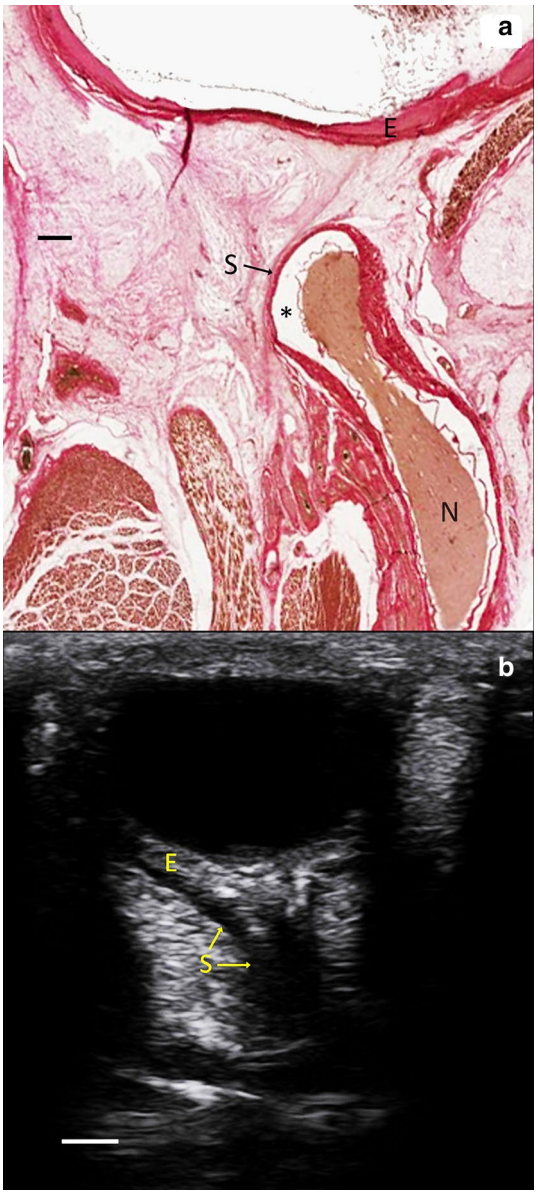

Fig. 1 Morphology of the optic nerve and nerve sheath in *Alligator mississippiensis*. **a** Frontal section through the optic nerve (N), nerve sheath (S), and sclera of the eye (E). The space between the nerve and nerve sheath (asterisk) is continuous with the subarachnoid space; expansion of this space is possible, in part, due to the loose connective tissue around the nerve sheath. **b** Ocular ultrasonogram illustrating the same level, and basic anatomy, indicated in **a**. The nerve sheath flares out as it integrates with the connective tissue on the medial surface of the eye. The distal expansion of the optic nerve sheath was particularly evident during head-down rotation. Scale bars in both images are 5 mm

passes through loose connective tissue, as they course away from the eye; the adjacent tissues do not suggest a structural limit on optic nerve sheath dilation (Fig. 1).

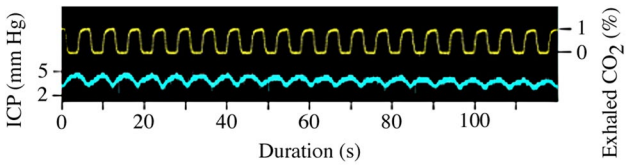

Fig. 2 Simultaneously recorded raw data traces of intracranial pressure (blue trace recorded from an implanted catheter and pressure transducer) and exhalatory CO_2 levels (yellow trace recorded from a gas analyzer). The steady pattern of the ventilator-driven tidal airflow is evident in the CO_2 traces and the same pattern is evident in the intracranial pressure trace

Gravitational gradients and intracranial pressure

The five *Alligator mississippiensis* had a mean intracranial pressure (ICP) of 4.2 mm Hg (s.d. = 0.04) and a mean optic nerve sheath diameter of 3.4 mm. The standard deviation of the resting optic nerve sheath diameter (0.35) was relatively large, reflecting the variation in nerve sheath diameter noted over time in every individual. The ICP recorded through the surgically implanted catheter frequently contained regular pulsations, which tracked the movements of the alligator (Fig. 2) driven by mechanical ventilation. These "ventilatory" pulsations increased the ICP by approximately 1.5 mm Hg.

When the alligator was rotated through discrete stages, there were clear transitions in ICP (Fig. 3a). During the same rotations, ocular ultrasonography demonstrated distinct changes in the size of the optic nerve sheath (Fig. 3b,c). When the quantitative changes in ICP and optic nerve sheath diameter during rotations were compared (Fig. 4), there was no significant difference in the slopes of the two lines ($Z = 1.074$, $\rho = 0.28$) and the two data sets had a correlation coefficient (r) of 0.978.

Rotating the alligator 15° created a mean change in ICP of 8.3 mm Hg (s.d. = 2.6), there was no significant difference ($t = 0.94$, $\rho = 0.187$) in the magnitude of pressure change between head-up (mean = 9.1 mm Hg, s.d. = 2.2) and head-down (mean = 7.6 mm Hg, s.d. = 2.5) rotations. There was a consistent pattern to the change in ICP during the 15° rotations (Fig. 5a). There was an initial rapid change in pressure (denoted by α in Fig. 5a) followed by a longer and more gradual change in ICP; curve fitting demonstrated that the longer gradual change could be consistently divided into two sections of nearly equal length (β and γ in Fig. 5a). There was no significant difference ($t = -0.04671$, $\rho = 0.482$) in the duration of the initial rapid change in ICP (mean durations of 5.26 and 5.29 s for head-down and head-up rotations, respectively). During both head-down and head-up rotations, the initial rapid change in ICP accounted for approximately 40% of the total pressure change (mean % of 37 for head-down and

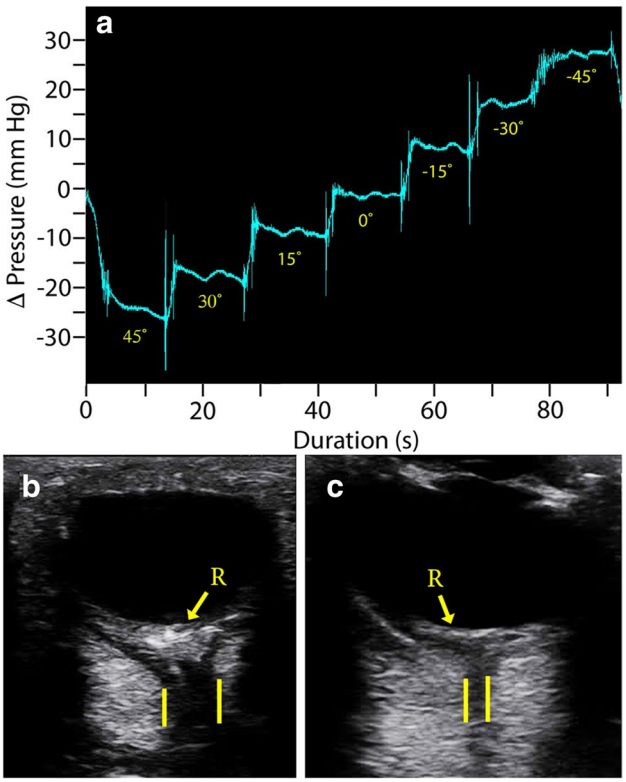

Fig. 3 Changes in intracranial pressure during rotation of *Alligator mississippiensis*. **a** Raw data trace of intracranial pressure (recorded from an implanted catheter and pressure transducer) taken, while the specimen transited through a series of head-up and head-down rotations. **b** Ocular ultrasonographic image of the retina (R) and optic nerve sheath (yellow lines) from an alligator during a 45° head-down rotation. **c** this image is at the same magnification and anatomical location as that shown in **b,** but was taken, while the specimen was in a 45° head-up rotation

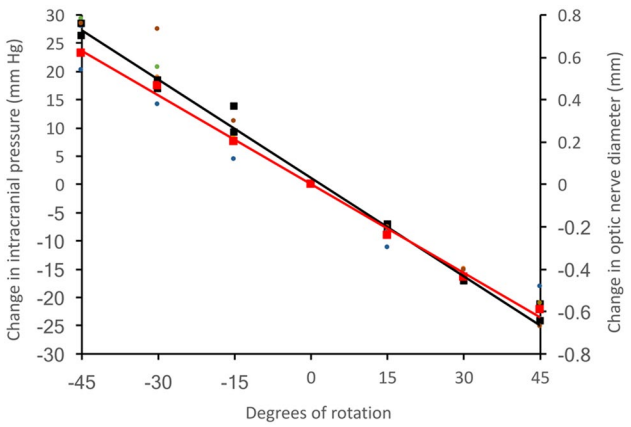

Fig. 4 Change in intracranial pressure of *Alligator mississippiensis* caused by orthostatic gradients. Intracranial pressure was recorded using both a surgically implanted catheter/pressure transducer (left vertical axis, mean values are indicated by the black squares) and ocular ultrasonography (right vertical axis, mean values are indicated by the red squares). There is no significant difference between the slopes of the two lines, and the two data sets have a correlation coefficient of 0.98

43 for head-up), with no significant difference between the directions of rotation ($t = -1.861$, $\rho = 0.50$).

The second phase of pressure change (β in Fig. 5a) accounted for 52% of total pressure change during both directions of rotation. There were significant differences among the phases (ANOVA for head-up $F = 63.93$, $\rho < 0.001$; head-down $F = 90.86$, $\rho < 0.001$) but in both cases, Tukey's post hoc analysis did not find significant difference between the amount of pressure change in the first two phases. When the rate of ICP change was compared, there were significant differences among the three phases (ANOVA for head-up $F = 127.3$, $\rho < 0.001$; head-down $F = 69.87$, $\rho < 0.001$); in both cases, Tukey's post hoc test found the rate of pressure change to be significantly greater during the first phase (α of Fig. 5a), but not different between the two subsequent phases.

When the ICP catheter data during rotations are plotted with the ocular sonographic measurements of the optic nerve sheath diameter (Fig. 5b), second-order polynomial curves provide the best fit to both data sets. Though both data sets were plotted on axes of relative change, the best fit curves, and many of the nerve sheath data points fall outside of the curve for the ICP catheter data.

Other influences on intracranial pressure

The jugular vein and common carotid artery were occluded (separately) and the animals rotated. Variation was still observed in the optic nerve sheath diameter (Fig. 6) performed on the same side as the occluded vessel, yet similar responses were found to the orthostatic gradient established by rotation. When the regression coefficients were averaged for all the alligators, there was no significant difference between the jugular occluded and carotid occluded responses to either head-up ($t = -1.54$, $\rho = 0.175$) or head-down ($t = -0.0448$, $\rho = 0.966$) rotation (Fig. 6).

Heating the snout of the alligator resulted in an increase in the diameter of the optic nerve sheath (Fig. 7a). In every individual, there was a positive regression relationship between narial temperature and nerve sheath diameter, and all of the regression coefficients were significantly different from zero. The regression coefficients ranged from 0.08 to 0.25, with a mean of 0.14 (s.d. = 0.07). Increasing the cephalic temperature of any of the specimens by 3 °C resulted in a larger increase in optic nerve sheath diameter than was observed during 15° head-down rotations.

Administration of epinephrine (0.1 mg/kg) into the triceps led to marked expansion in the size of the optic nerve sheath, as measured with ocular ultrasonography (Fig. 7b). The expansion of the nerve sheath started shortly after the

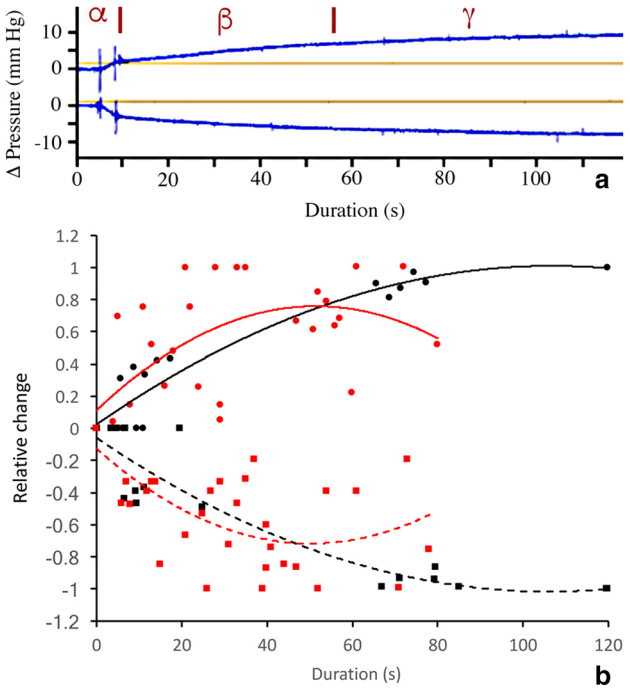

Fig. 5 Impact of gravitational gradients on intracranial pressure. **a** Two raw data tracings from the same specimen of *Alligator mississippiensis* showing the temporal pattern of change in intracranial pressure (recorded from an implanted catheter/pressure transducer) when the animal is rotated to 15° head-down (upper trace) and 15° head-up (lower trace). The temporal pattern of the response could be divided into three phases or segments (α, β, γ), the boundaries of which are indicated by the vertical red lines. **b** Pooled data showing the head-up (square data points and dashed lines) and head-down (round data points and solid lines) rotations, with ICP measured from catheter/transducer (black) or ocular ultrasonography (red). For all the data sets, the best fit line was a 2nd order polynomial. Note that the optic nerve sheath expands faster than the rate of ICP increase recorded with the catheter

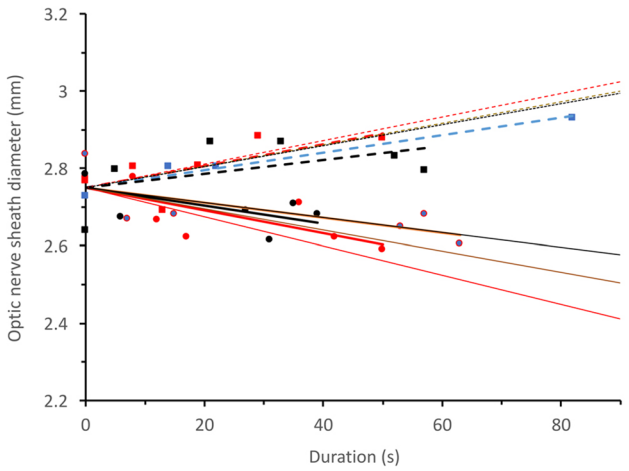

Fig. 6 Effect of vascular occlusion on intracranial pressure in *Alligator mississippiensis*. Gravitation gradients were created by 15° rotations in both the head-up (round data points, solid thick lines) and head-down (square data points, dashed thick lines) directions. Data points shown are from a single individual, and show baseline (no occlusion) trials (black), trials with unilateral common carotid occlusion (red), and trials with unilateral jugular occlusion (blue). Best fit means are shown for the pooled data across the five specimens during head-up (thin solid lines) and head-down (dashed thin lines). Note that the unilateral occlusion of the common carotid (red) or jugular (blue) do not result in significant differences in optic nerve sheath diameter

injection of the epinephrine, and peaked at approximately 150 s post-injection (Fig. 7b). When epinephrine was administered during the non-invasive trials (in the absence of isoflurane), it resulted in a mean increase 1.9 mm in optic nerve sheath diameter (s.d. = 0.94); in the presence of isoflurane, the administration of epinephrine resulted in the optic nerve sheath diameter increasing by a mean of 1.3 mm (s.d. = 0.26). The presence of isoflurane did not ($t = 1.43$, $\rho = 0.195$) produce a significant difference on the optic nerve sheath's response to epinephrine.

Rotation of the alligators always resulted in a transitory low-level increase in heart rate, but compensatory bradycardia or tachycardia was never observed, even when the animals were held at 45° rotations. Representative raw data from a 30° head-up rotation are shown in Fig. 8. While there was variation in the instantaneous heart rate (blue circles), and the best fit line was a second-order polynomial, the total variation was in the range of 3 bpm and the rotation ends at the same heart rate as it began. In contrast, the optic nerve sheath diameter exhibited a continuous linear decrease (red squares, Fig. 8) throughout the duration of the head-up rotation. While the direction of optic nerve sheath changed between head-up and head-down rotations, this same pattern of linear change in the nerve sheath coupled with no significant change in heart rate was observed during every gravitational gradient. Accordingly, this study found no correlation between intracranial pressure and heart rate in *Alligator*.

Discussion

Gravitational gradients and intracranial pressure

Gravitational (orthostatic) gradients produced marked changes in both the intracranial pressure and optic nerve sheath diameter (Fig. 3). The significant relationship between the intracranial pressure and optic nerve sheath in anesthetized *Alligator* (Fig. 4) has been reported from multiple earlier human studies (Geeraerts et al. 2008; Soldatos et al. 2008; Moretti and Pizzi 2009). In the alligator, gravitational gradients produced a phasic change in ICP (Fig. 5), which has not been previously reported. The first two phases (α and β of Fig. 5a) represent roughly 90% of the pressure change, but have significantly different rates of change. We

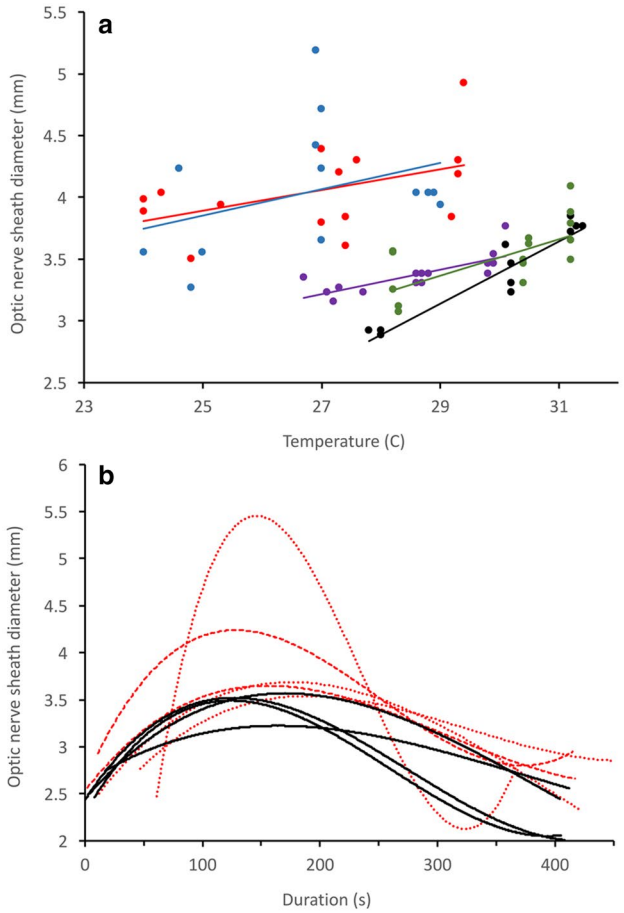

Fig. 7 Influences on the diameter of the optic nerve sheath of *Alligator mississippiensis*. **a** In each individual (color coded) the application of heat to the dorsum of the snout caused an increase in narial temperature and an increase in optic nerve sheath diameter. **b** Black lines are trials in which the animal was anesthetized with isoflurane prior to administration of the epinephrine, red lines are trials, where the epinephrine was given without isoflurane. In all cases the optic nerve sheath increased in diameter approximately 150 s after the IM introduction of epinephrine into the triceps

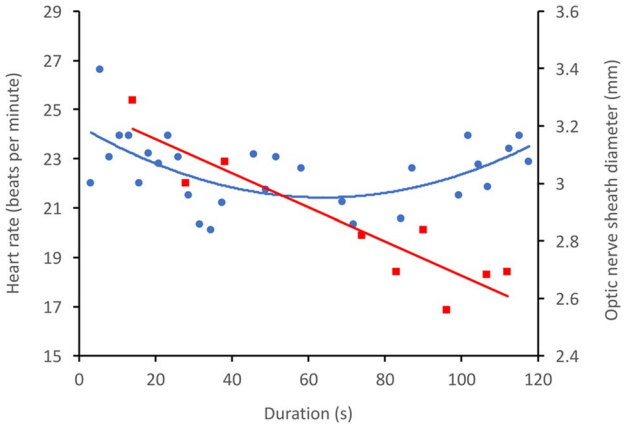

Fig. 8 Relationship of instantaneous heart rate to intracranial pressure in *Alligator mississippiensis*. Data shown are from a 30 head-up rotation of one alligator; in all of the rotation trials the heart rate (blue points and line) showed no barostatic response regardless of magnitude or direction of rotation. In contrast, the intracranial pressure, as measure by the optic nerve sheath using ocular ultrasonography (red points and line), showed a typically linear response that tracked the magnitude and direction of the animal's rotation

hypothesize that the initial phase of pressure change (α in Fig. 5a) reflects the bulk flow of CSF in the subarachnoid space, while the later longer phase (β in Fig. 5a) reflects the movement of CSF across the reptilian tela choroidea over the fourth ventricle. While marker studies have shown exchange between the ventricular and subarachnoid CSF (Heisey 1970; Jones 1980), and the tela choroidea of the fourth ventricle has been shown to includes small pores in some lower vertebrates (Jones 1979), and the nature of this system in crocodilians remains unknown.

The optic nerve sheath diameter exhibited a faster rate of change than was recorded directly from the catheter (Fig. 5b); the temporal relationship between these two does not appear to have been previously studied. We hypothesize that while the nerve sheath contains CSF that is continuous with that of the subarachnoid (Fig. 1), the marked differences in the tissues surrounding these two CSF-filled spaces result in differences in compliance and pressure–volume Index, which could account for the temporal pattern observed in *A. mississippiensis* (Andrews and Citerio 2004; Alperin et al. 2006).

Other influences on intracranial pressure

The presence of pulsations within the ICP (Fig. 2) has long been recognized (Reitan 1941), as has the distinction between arterial and ventilatory pulsation patterns (Dardenne et al. 1969; Kirkness et al. 2000). The CSF pulsations recorded from anesthetized *A. mississippiensis* were clearly synchronized to the ventilatory pattern. The magnitude of these pulsations (approximately 2 mm Hg) though roughly 1/3 of what is typically seen in humans was large enough to discount catheter movement artifact, as this would necessitate the 500 ml tidal volume elevating a 1.5 m alligator by over 1 cm. The presence of these ventilatory CSF pulsations is suggestive of changes in "intrathoracic" pressure (Martin and Loth 2009); in humans, the intrathoracic pressure is communicated to the CSF by way of venous pressure (Foltz et al. 1990; Dreha-Kulaczewski et al. 2015), though the functional link between intrathoracic and intracranial pressure is unclear in *Alligator*. In the present study, no CSF pulsations were found to correlate with heart rate, though this functional connection is well known in humans and other mammals (Wagshul et al. 2011). ICP pulsations can be altered by anesthesia and artificial ventilation (Levinger and Kedem 1972); it is not clear if these factors influenced

the absence of vascular pulse waves in the CSF of *Alligator*, or if the apparent lack of these pulses is reflective of the reptilian brain and/or meningeal morphology.

Our understanding of the fluid dynamics of the brain, both at the interstitial and bulk-flow levels, is still developing (Hladky and Barrand 2014; Linninger et al. 2016). Previous studies have explored the ICP's relationship to carotid (arterial) flow (Iliff et al. 2013; Shi et al. 2018), cerebral blood flow (Steiner and Andrews 2006), and venous return (Stoquart-ElSankari et al. 2009; Zamboni et al. 2010). In contrast to these earlier human/mammalian studies, we found that neither occlusion of the cerebral arterial supply or venous drainage (Fig. 6), nor heart rate (Fig. 8), had an effect on ICP. This is surprising given that an earlier study found significant changes in the luminal volume of the common carotid artery and jugular vein in response to orthostatic gradients (Knoche et al. 2019); the surgical occlusion of these vessels was designed to alter and/or prevent these shifts in blood distribution. The absence of any impact on ICP may reflect the short-term nature of the vascular challenges used in the present study. At the same time, given the nature of the reportedly avascular reptilian arachnoid (Zajicova 1975), it seems likely that the dynamic balance between blood and CSF is based on different mechanics in *Alligator*.

The response to epinephrine affords a clear indicator that the mechanics of cerebral fluid balance are different in *Alligator* than in humans. In humans, the administration of epinephrine (in clinically relevant doses) does not produce a significant change in ICP (Myburgh et al. 1998; Malkinson et al. 1985; Ract and Vigue 2001; Steiner et al. 2004). In alligators, the IM administration of epinephrine produced a transitory "spike" in ICP (Fig. 7b); the magnitude of the epinephrine-induced increase in ICP (as documented by optic nerve sheath dilation) was greater than what was found during 45° head-down rotations. Though beyond the scope of the present study, we hypothesize that differential receptor expression in *Alligator* results in epinephrine increasing CSF secretion into the ventricles and/or decreases CSF absorption into the venous system, leading to the distinctive curved rate of ICP change shown in Fig. 7b. Complicating this interpretation is the fact that the non-anesthetized animals (red lines of Fig. 7b) showed a more pronounced (though not significantly greater) response to epinephrine than the anesthetized animals (black lines in Fig. 7b). In humans and other mammals, isoflurane increases cerebral blood flow (Maekawa et al. 1986; Sicard et al. 2003; Tetrault et al. 2008) and so would have been expected to produce the opposite effect from the one observed.

Reptiles perform behavioral and physiological thermoregulation; one means for the latter is shunting of venous blood (Baker et al. 1972). Reptiles have multiple cephalic venous sinus systems (Bruner 1907; Porter and Witmer 2015); the peripheral portion of this complex includes an orbital venous plexus that is in close proximity to the optic nerve sheath (Porter et al. 2016). During shunting, changes in the orbital venous pressure are substantial enough to displace (bulge) the eyes laterally (Reyes-Olivares et al. 2016) and, in *Phrynosoma*, to eject blood, under pressure, as a defensive mechanism (Burleson 1942). We hypothesized that the direct application of external heat to the head would lead to blood being shunted away from the peripheral venous distribution, causing an increase in central venous pressure and an associated increase in ICP. In every (non-anesthetized) alligator, the application of peripheral heat to the snout resulted in a significant increase in ICP, as measured by optic nerve sheath diameter (Fig. 7a). This study did not directly measure the flow of venous blood, nor did we control for any heat-related change in compliance of tissues surrounding the optic nerve sheath (Carmelo et al. 2002; Porter et al. 2016). It is noteworthy that of the vascular perturbations that we studied, only the application of superficial heat had a significant impact on ICP.

The meninges of the American alligator (*Alligator mississippiensis*) have similarities and differences to the human and mammalian meninges. While intracranial pressure data collected from the optic nerve sheath and cranial subarachnoid space were found to be highly correlated, there was a phasic response of the intracranial pressure to orthostatic orthostatic gradients, and a lack of pressure response to vascular perturbation. The alligator system may offer unique opportunities to examine the relationships between membrane receptors and CSF flow.

Acknowledgements We thank Dr. Ruth Elsey of the Louisiana Department of Wildlife and Fisheries, and Dr. Peter Kondrashov for his continued support of this research program.

Compliance with ethical standards

Ethical approval The husbandry and use of the live alligators followed all applicable federal guidelines, and was approved by the Institutional Animal Care and Use Committee of A.T. Still University (Protocols #208 and #209).

References

Alperin N, Mazda M, Lichtor T, Lee S (2006) From cerebrospinal fluid pulsation to noninvasive intracranial compliance and pressure measured by MRI flow studies. Curr Med Imag Rev 2:117–129

Andrews P, Citerio G (2004) Intracranial pressure. Part one: historical overview and basic concepts. Int Care Med 30:1730–1733

Ariens Kappers C (1926) The meninges in lower vertebrates compared with those in mammals. Arch Neurol Psychiatry 15:281–296

Ariens Kappers C, Huber G, Crosby E (1960) The comparative anatomy of the nervous system of vertebrates including man. Hafner, New York

Baker L, Weathers W, White F (1972) Temperature induced peripheral blood flow changes in lizards. J Comp Physiol 80:312–323

Brocklehurst R, Moritz S, Codd J, Sellers W, Brainerd E (2017) Rib kinematics during lung ventilation in the American alligator (*Alligator mississippiensis*): an XROMM analysis. J Exp Biol 220:3181–3190

Bruner H (1907) On the cephalic veins and sinuses of reptiles, with a description of a mechanism for raising the venous blood-pressure in the head. Am J Anat 7:1–117

Burleson G (1942) The source of blood ejected from the eyes of horned lizards. Copeia 1942:246–248

Carmelo A, Ficola A, Fravolini M, La Cava M, Maira G et al (2002) ICP and CBF regulation: effect of the decompressive craniectomy. In: Czosnyka M, Pickard J, Kirkpatrick P, Smielewski P, Hutchinson P (eds) Intracranial pressure and brain biochemical monitoring. Springer, New York, pp 109–111

Carney N, Totten A, O'Reilly C, Ullman J, Hawryluk G et al (2017) Guidelines for the management of severe traumatic brain injury, 4th edition. Neurosurgery 80:6–15

Claessens L (2009) A cineradiographic study of lung ventilation in *Alligator mississippiensis*. J Exp Zool 311A:563–585

Cooley S, Scrivani P, Thompson M, Irby N, Divers T et al (2015) Correlations among ultrasonographic measurements of optic nerve sheath diameter, age, and body weight in clinically normal horses. Vet Radiol Ultrasound 57:49–57

Cserr H, Bundgaard M (1984) Blood-brain interfaces in vertebrates: a comparative approach. Am J Physiol 246:R277–R288

Dardenne G, Dereymaeker A, Lacheron J (1969) Cerebrospinal fluid pressure and pulsatility. An experimental study of circulatory and respiratory influences in normal and hydrocephalic dogs. Eur Neurol 2:192–216

Dreha-Kulaczewski S, Joseph A, Merboldt K-D, Ludwig H-C, Gartner J et al (2015) Inspiration is the major regulator of human CSF flow. J Neurosci 35:2485–2491

Ferguson N, Shein S, Kochanek P, Luther J, Wisniewski S et al (2016) Intracranial hypertension and cerebral hypoperfusion in children with severe traumatic brain injury: thresholds and burden in accidental and abusive insults. Pediatr Crit Care Med 17:444–450

Fernando S, Tran A, Cheng W, Rochwerg B, Taljaard M et al (2019) Diagnosis of elevated intracranial pressure in critically ill adults: systematic review and meta-analysis. BMJ 366:14225

Foltz E, Blanks J, Yonemura K (1990) CSF pulsatility in hydrocephalus: respiratory effect on pulse wave slope as an indicator of intracranial compliance. Neurol Res 12:67–74

Gatson B, Goe A, Granone T, Wellehan J (2017) Intramuscular epinephrine results in reduced anesthetic recovery time in American alligators (*Alligator mississippiensis*) undergoing isoflurane anesthesia. J Zoo Wildl Med 48:55–61

Geeraerts T, Merceron S, Benhamou D, Vigue B, Duranteau J (2008) Non-invasive assessment of intracranial pressure using ocular sonography in neurocritical care patients. Crit Care 12:P117

Hansen H, Helmke K (1996) The subarachnoid space surrounding the optic nerves. An ultrasound study of the optic nerve sheath. Surg Radiol Anat 18:323–328

Hansen H, Helmke K, Kunze K (1994) Optic nerve sheath enlargement in acute intracranial hypertension. Neuro Ophthalmol 14:345–354

Heisey S (1970) Cerebrospinal and extracellular fluid spaces in turtle brain. Am J Physiol 219:1564–1567

Hladky S, Barrand M (2014) Mechanisms of fluid movement into, through and out of the brain: Evaluation of the evidence. Fluids Barriers CNS. http://www.fluidsbarrierscns.com/content/11/1/26

Iliff J, Wang M, Zeppenfeld D, Venkataraman A, Plog B et al (2013) Cerebral arterial pulsation drives perivascular CSF-Interstitial fluid exchange in the murine brain. J Neurosci 33:18190–18199

Jagannathan J, Okonkwo D, Yeoh H, Dumont A, Saulle D et al (2008) Long-term outcomes and prognostic factors in pediatric patients with severe traumatic brain injury and elevated intracranial pressure. J Neurosurg Pediatrics 2:240–249

Jones H (1978) Continuity between the ventricular and subarachnoid cerebrospinal fluid in amphibian, *Rana pipiens*. Cell Tissue Res 195:153–167

Jones H (1979) Fenestration of the epithelium lining the roof of the fourth cerebral ventricle in amphibia. Cell Tissue Res 198:129–136

Jones H (1980) Circulation of marker substances in the cerebrospinal fluid of an amphibian, *Rana pipiens*. Cell Tissue Res 195:153–167

Killer H, Laeng H, Flammer J, Groscurth P (2003) Architecture of arachnoid trabeculae, pillars, and septa in the subarachnoid space of the human optic nerve: anatomy and clinical considerations. Br J Ophthalmol 87:777–781

Kirkness C, Mitchell P, Burr R, March K, Newell D (2000) Intracranial pressure waveform analysis: clinical and research implications. J Neuro Nurs 32:271–277

Knoche L, Young BA, Kondrashova T (2019) The influence of gravitational gradients on the American alligator (*Alligator mississippiensis*). Anat Physiol Curr Res. https://doi.org/10.35248/2161-0940.19.9.318

Komut E, Kozaci N, Sonmez B, Yilmaz F, Komut S, et al. (2016) Bedside sonographic measurement of optic nerve sheath diameter as a predictor of intracranial pressure in ED. Am J Emerg Med 34:963–967

Levinger I, Kedem J (1972) Further mechanisms determining respiratory waves in the cerebrospinal fluid pressure. Eur Neurol 8:325–332

Linninger A, Tangen K, Hsu C-Y, Frim D (2016) Cerebrospinal fluid mechanics and its coupling to cerebrovascular dynamics. Ann Rev Fluid Mech 48:219–257

Liu D, Kahn M (1993) Measurement and relationship of subarachnoid pressure of the optic nerve to intracranial pressures in fresh cadavers. Am J Opthalmol 116:548–556

Maekawa T, Tommasino C, Shapiro H, Keifer-Goodman J, Kohlenberger R (1986) Local cerebral blood flow and glucose utilization during isoflurane anesthesia in the rat. Anesthesiology 65:144–151

Malkinson T, Cooper K, Veale W (1985) Induced changes in intracranial pressure in the anesthetized rat and rabbit. Brain Res Bull 15:321–328

Martin B, Loth F (2009) The influence of coughing on cerebrospinal fluid pressure in an in vitro syringomyelia model with spinal subarachnoid space stenosis. Fluids Barriers CNS. https://doi.org/10.1186/1743-8454-6-17

Moretti R, Pizzi B (2009) Optic nerve ultrasound for detection of intracranial hypertension in intracranial hemorrhage patients: confirmation of previous findings in a different patient population. J Neurosurg Anesth 21:16–20

Myburgh J, Upton R, Grant C, Martinez A (1998) A comparison of the effects of norepinephrine, epinephrine, and dopamine on cerebral blood flow and oxygen utilisation. In: Marmarou A, Bullock R, Avezaat C, Baethmann A, Becker D, Brock M, Hoff J, Nagai H, Reulen H-J, Teasdale G (eds) Intracranial pressure and neuromonitoring in brain injury. Springer, Vienna, pp 19–21

Porter W, Witmer L (2015) Vascular patterns in Iguanas and other squamates: blood vessels and sites of thermal exchange. PLoS One. https://doi.org/10.1371/journal.pone.0139215

Porter W, Sedimayr J, Witmer L (2016) Vascular patterns in the heads of crocodilians: blood vessels and sites of thermal exchange. J Anat 229:800–824

Ract C, Vigue B (2001) Comparison of the cerebral effects of dopamine and norepinephrine in severely head-injured patients. Int Care Med 27:101–106

Raffiz M, Abdullah J (2017) Optic nerve sheath diameter measurement: a means of detecting raised ICP in adult traumatic and non-traumatic neurosurgical patients. Am J Emerg Med 35:150–153

Rajajee V, Vanaman M, Fletcher J, Jacobs T (2011) Optic nerve ultrasound for the detection of raised intracranial pressure. Neurocritic Care 15:506–515

Reitan H (1941) On movements of fluid inside the cerebrospinal space. Arch Radiol 22:762–779

Reyes-Olivares C, Rain-Garrido I, Labra A (2016) The eye-bulging in *Liolaemus* lizards (Weigmann 1843). Gayana 80:129–132

Shi Y, Thrippleton M, Marshall I, Wardlaw J (2018) Intracranial pulsatility in patients with cerebral small vessel disease: a systematic review. Clin Sci 132:151–171

Sicard K, Shen Q, Brevard M, Sullivan R, Ferris C et al (2003) Regional cerebral blood flow and BOLD responses in conscious and anesthetized rats under basal and hypercapnic conditions: implications for functional MRI studies. J Cereb Blood Flow Metabol 23:472–481

Smith J, Fletcher D, Cooley S, Thompson M (2018) Transpalpebral ultrasonographic measurement of the optic nerve sheath diameter in healthy dogs. J Vet Emerg Crit Care 28:31–38

Soldatos T, Karakitsos D, Chatzimichail K, Papathanasiou M, Gouliamos A et al (2008) Optic nerve sonography in the diagnostic evaluation of adult brain injury. Crit Care 12:R67

Stark D (1969) Cranio-cerebral relations in recent reptiles. In: Gans C, Northcutt C, Ulinski P (eds) Biology of the reptilia, vol 9. Academic Press, New York, pp 1–38

Steiner L, Andrews P (2006) Monitoring the injured brain: ICP and CBF. Br J Anaesth 97:26–38

Steiner L, Johnston A, Czosnyka M, Chatfield D, Salvador R et al (2004) Direct comparison of cerebrovascular effects of norepinephrine and dopamine in head-injured patients. Crit Care Med 32:1049–1054

Stoquart-ElSankari S, Lehmann P, Villette A, Czosnyka M, Meyer M-E et al (2009) A phase-contrast MRI study of physiologic cerebral venous flow. J Cereb Blood Flow Metab 29:1208–1215

Strumwasser A, Kwan R, Yeung L, Mirallor E, Ereso A et al (2011) Sonographic optic nerve sheath diameter as an estimate of intracranial pressure in adult trauma. J Surg Res 170:265–271

Tetrault S, Chever O, Sik A, Amzica F (2008) Opening of the blood-brain barrier during isoflurane anaesthesia. Eur J Neurosci 28:1330–1341

Wagshul M, Eide P, Madsen J (2011) The pulsating brain: a review of experimental and clinical studies of intracranial pulsatility. Fluids Barriers CNS. https://doi.org/10.1186/2045-8118-8-5

Witmer L, Ridgely R (2008) The paranasal air sinus of predatory and armored dinosaurs (Archosauria: Therapoda and Ankylosauria) and their contribution to cephalic structure. Anat Rec 291:1362–1388

Yang X-Y, Yang J-P, Zhu L-P, Pan R-H, Huang Y-N et al (2017) Transorbital ultrasound measurement of optic nerve sheath diameter in normal rabbits. Int J Clin Exp Med 10:13412–13418

Zajicova A (1975) Comparative morphology of the meninges of Amphibians and Reptiles. Folia Morphol 23:56–64

Zamboni P, Menegatti E, Weinstock-Guttman B, Schirda C, Cox J et al (2010) CSF dynamics and brain volume in multiple sclerosis are associated with extracranial venous flow anomalies: a pilot study. Int Angiol 29:140–148

Publisher's Note Springer Nature remains neutral with regard to jurisdictional claims in published maps and institutional affiliations.